

# Search for $Z^0$ Decays to two Leptons and a Charged Particle-Antiparticle Pair

DELPHI Collaboration



## Abstract

Based on a sample equivalent to 365,000 hadronic  $Z^0$  decays, the search in DELPHI data for pairs of leptons accompanied by a pair of charged particles is described. A total of 11 events were found in the electron channel, 9 in the muon channel and 7 in the tau channel. Results on lepton pairs with a radiated photon are also presented. The data from all channels are compatible with the expectations from standard processes. However, one event was found in the tau channel with an unusually high mass of the charged particle pair.

(Submitted to Nuclear Physics B)

P. Abreu<sup>20</sup>, W. Adam<sup>7</sup>, T. Adye<sup>37</sup>, E. Agasi<sup>30</sup>, R. Aleksan<sup>39</sup>, G.D. Alekseev<sup>14</sup>, A. Algeri<sup>13</sup>, P. Allen<sup>49</sup>, S. Almehed<sup>23</sup>,  
 S.J. Alvsvaag<sup>4</sup>, U. Amaldi<sup>7</sup>, A. Andreazza<sup>27</sup>, P. Antilogus<sup>24</sup>, W-D. Apel<sup>15</sup>, R.J. Apsimon<sup>37</sup>, Y. Arnoud<sup>39</sup>,  
 B. Åsman<sup>45</sup>, J-E. Augustin<sup>18</sup>, A. Augustinus<sup>30</sup>, P. Baillon<sup>7</sup>, P. Bambade<sup>18</sup>, F. Barao<sup>20</sup>, R. Barate<sup>12</sup>, G. Barbiellini<sup>47</sup>,  
 D.Y. Bardin<sup>14</sup>, G.J. Barker<sup>34</sup>, A. Baroncelli<sup>41</sup>, O. Barring<sup>7</sup>, J.A. Barrio<sup>25</sup>, W. Bartl<sup>50</sup>, M.J. Bates<sup>37</sup>, M. Battaglia<sup>13</sup>,  
 M. Baubillier<sup>22</sup>, K-H. Becks<sup>52</sup>, C.J. Beeston<sup>34</sup>, M. Begalli<sup>36</sup>, P. Beilliere<sup>6</sup>, Yu. Belokopytov<sup>43</sup>, P. Beltran<sup>9</sup>,  
 D. Benedic<sup>8</sup>, A.C. Benvenuti<sup>5</sup>, M. Berggren<sup>18</sup>, D. Bertrand<sup>2</sup>, F. Bianchi<sup>46</sup>, M.S. Bilenky<sup>14</sup>, P. Billoir<sup>22</sup>, J. Bjarne<sup>23</sup>,  
 D. Bloch<sup>8</sup>, S. Blyth<sup>34</sup>, V. Bocci<sup>38</sup>, P.N. Bogolubov<sup>14</sup>, T. Bolognese<sup>39</sup>, M. Bonesini<sup>27</sup>, W. Bonivento<sup>27</sup>, P.S.L. Booth<sup>21</sup>,  
 G. Borisov<sup>43</sup>, H. Borner<sup>7</sup>, C. Bosio<sup>41</sup>, B. Bostjancic<sup>44</sup>, S. Bosworth<sup>34</sup>, O. Botner<sup>48</sup>, E. Boudinov<sup>43</sup>, B. Bouquet<sup>18</sup>,  
 C. Bourdarios<sup>18</sup>, T.J.V. Bowcock<sup>21</sup>, M. Bozzo<sup>11</sup>, S. Braibant<sup>2</sup>, P. Branchini<sup>41</sup>, K.D. Brand<sup>35</sup>, R.A. Brenner<sup>7</sup>,  
 H. Briand<sup>22</sup>, C. Bricman<sup>2</sup>, R.C.A. Brown<sup>7</sup>, N. Brummer<sup>30</sup>, J-M. Brunet<sup>6</sup>, L. Bugge<sup>32</sup>, T. Buran<sup>32</sup>, H. Burmeister<sup>7</sup>,  
 J.A.M.A. Buytaert<sup>7</sup>, M. Caccia<sup>7</sup>, M. Calvi<sup>27</sup>, A.J. Camacho Rozas<sup>42</sup>, R. Campion<sup>21</sup>, T. Camporesi<sup>7</sup>, V. Canale<sup>38</sup>,  
 F. Cao<sup>2</sup>, F. Carena<sup>7</sup>, L. Carroll<sup>21</sup>, C. Caso<sup>11</sup>, M.V. Castillo Gimenez<sup>49</sup>, A. Cattai<sup>7</sup>, F.R. Cavallo<sup>5</sup>, L. Cerrito<sup>38</sup>,  
 V. Chabaud<sup>7</sup>, A. Chan<sup>1</sup>, Ph. Charpentier<sup>7</sup>, L. Chaussard<sup>18</sup>, J. Chauveau<sup>22</sup>, P. Checchia<sup>35</sup>, G.A. Chelkov<sup>14</sup>,  
 L. Chevalier<sup>39</sup>, P. Chliapnikov<sup>43</sup>, V. Chorowicz<sup>22</sup>, J.T.M. Chrin<sup>49</sup>, P. Collins<sup>34</sup>, J.L. Contreras<sup>25</sup>, R. Contri<sup>11</sup>,  
 E. Cortina<sup>49</sup>, G. Cosme<sup>18</sup>, F. Couchot<sup>18</sup>, H.B. Crawley<sup>1</sup>, D. Crennell<sup>37</sup>, G. Crosetti<sup>11</sup>, M. Crozon<sup>6</sup>,  
 J. Cuevas Maestro<sup>33</sup>, S. Czellar<sup>13</sup>, E. Dahl-Jensen<sup>28</sup>, B. Dalmagne<sup>18</sup>, M. Dam<sup>32</sup>, G. Damgaard<sup>28</sup>, G. Darbo<sup>11</sup>,  
 E. Daubie<sup>2</sup>, A. Daum<sup>15</sup>, P.D. Dauncey<sup>34</sup>, M. Davenport<sup>7</sup>, P. David<sup>22</sup>, J. Davies<sup>21</sup>, W. Da Silva<sup>22</sup>, C. Defoix<sup>6</sup>,  
 P. Delpierre<sup>6</sup>, N. Demaria<sup>46</sup>, A. De Angelis<sup>47</sup>, H. De Boeck<sup>2</sup>, W. De Boer<sup>15</sup>, C. De Clercq<sup>2</sup>, M.D.M. De Fez Laso<sup>49</sup>,  
 N. De Groot<sup>30</sup>, C. De La Vaissiere<sup>22</sup>, B. De Lotto<sup>47</sup>, A. De Min<sup>27</sup>, H. Dijkstra<sup>7</sup>, L. Di Ciaccio<sup>38</sup>, J. Dolbeau<sup>6</sup>,  
 M. Donszelmann<sup>7</sup>, K. Doroba<sup>51</sup>, M. Dracos<sup>7</sup>, J. Drees<sup>52</sup>, M. Dris<sup>31</sup>, Y. Dufour<sup>7</sup>, F. Dupont<sup>12</sup>, D. Edsall<sup>1</sup>, L-O. Eek<sup>48</sup>,  
 P.A.-M. Eerola<sup>7</sup>, R. Ehret<sup>15</sup>, T. Ekelof<sup>48</sup>, G. Ekspong<sup>45</sup>, A. Elliot Peisert<sup>35</sup>, J-P. Engel<sup>8</sup>, N. Ershaidat<sup>22</sup>,  
 D. Fassouliotis<sup>31</sup>, M. Feindt<sup>7</sup>, M. Fernandez Alonso<sup>42</sup>, A. Ferrer<sup>49</sup>, T.A. Filippas<sup>31</sup>, A. Firestone<sup>1</sup>, H. Foeth<sup>7</sup>,  
 E. Fokitis<sup>31</sup>, F. Fontanelli<sup>11</sup>, K.A.J. Forbes<sup>21</sup>, J-L. Fousset<sup>26</sup>, S. Francon<sup>24</sup>, B. Franek<sup>37</sup>, P. Frenkiel<sup>6</sup>, D.C. Fries<sup>15</sup>,  
 A.G. Frodesen<sup>4</sup>, R. Fruhwirth<sup>50</sup>, F. Fulda-Quenzer<sup>18</sup>, K. Furnival<sup>21</sup>, H. Furstenau<sup>15</sup>, J. Fuster<sup>7</sup>, D. Gamba<sup>46</sup>,  
 C. Garcia<sup>49</sup>, J. Garcia<sup>42</sup>, C. Gaspar<sup>7</sup>, U. Gasparini<sup>35</sup>, Ph. Gavillet<sup>7</sup>, E.N. Gazis<sup>31</sup>, J-P. Gerber<sup>8</sup>, P. Giacomelli<sup>7</sup>,  
 R. Gokheli<sup>51</sup>, B. Golob<sup>44</sup>, V.M. Golovatyuk<sup>14</sup>, J.J. Gomez Y Cadenas<sup>7</sup>, G. Gopal<sup>37</sup>, L. Gorn<sup>1</sup>, M. Gorski<sup>51</sup>,  
 V. Gracco<sup>11</sup>, A. Grant<sup>7</sup>, F. Grard<sup>2</sup>, E. Graziani<sup>41</sup>, G. Grosdidier<sup>18</sup>, E. Gross<sup>7</sup>, P. Grosse-Wiesmann<sup>7</sup>, B. Grossetete<sup>22</sup>,  
 S. Gumenyuk<sup>43</sup>, J. Guy<sup>37</sup>, U. Haedinger<sup>15</sup>, F. Hahn<sup>52</sup>, M. Hahn<sup>15</sup>, S. Haider<sup>30</sup>, A. Hakansson<sup>23</sup>, A. Hallgren<sup>48</sup>,  
 K. Hamacher<sup>52</sup>, G. Hamel De Monchenault<sup>39</sup>, W. Hao<sup>30</sup>, F.J. Harris<sup>34</sup>, V. Hedberg<sup>23</sup>, T. Henkes<sup>7</sup>, J.J. Hernandez<sup>49</sup>,  
 P. Herquet<sup>2</sup>, H. Herr<sup>7</sup>, T.L. Hessing<sup>21</sup>, I. Hietanen<sup>13</sup>, C.O. Higgins<sup>21</sup>, E. Higon<sup>49</sup>, H.J. Hilke<sup>7</sup>, S.D. Hodgson<sup>34</sup>,  
 T. Hofmohl<sup>51</sup>, S-O. Holmgren<sup>45</sup>, D. Holthuisen<sup>30</sup>, P.F. Honore<sup>6</sup>, J.E. Hooper<sup>28</sup>, M. Houlden<sup>21</sup>, J. Hrubec<sup>50</sup>, K. Huet<sup>2</sup>,  
 P.O. Hulth<sup>45</sup>, K. Hultqvist<sup>45</sup>, P. Ioannou<sup>3</sup>, P-S. Iversen<sup>4</sup>, J.N. Jackson<sup>21</sup>, P. Jalocho<sup>16</sup>, G. Jarlskog<sup>23</sup>, P. Jarry<sup>39</sup>,  
 B. Jean-Marie<sup>18</sup>, E.K. Johansson<sup>45</sup>, D. Johnson<sup>21</sup>, M. Jonker<sup>7</sup>, L. Jonsson<sup>23</sup>, P. Juillot<sup>8</sup>, G. Kalkanis<sup>3</sup>, G. Kalmus<sup>37</sup>,  
 F. Kapusta<sup>22</sup>, M. Karlsson<sup>7</sup>, E. Karvelas<sup>9</sup>, S. Katsanevas<sup>3</sup>, E.C. Katsofisis<sup>31</sup>, R. Keranen<sup>7</sup>, J. Kesteman<sup>2</sup>,  
 B.A. Khomenko<sup>14</sup>, N.N. Khovanski<sup>14</sup>, B. King<sup>21</sup>, N.J. Kjaer<sup>7</sup>, H. Klein<sup>7</sup>, A. Klovning<sup>4</sup>, P. Kluit<sup>30</sup>, A. Koch-Mehrin<sup>52</sup>,  
 J.H. Koehne<sup>15</sup>, B. Koene<sup>30</sup>, P. Kokkinias<sup>9</sup>, M. Koratzinos<sup>32</sup>, A.V. Korytov<sup>14</sup>, V. Kostioukhine<sup>43</sup>, C. Kourkoumelis<sup>3</sup>,  
 O. Kouznetsov<sup>14</sup>, P.H. Kramer<sup>52</sup>, C. Kreuter<sup>15</sup>, J. Krolikowski<sup>51</sup>, I. Kronkvist<sup>23</sup>, U. Kruener-Marquis<sup>52</sup>,  
 W. Krupinski<sup>16</sup>, K. Kulka<sup>48</sup>, K. Kurvinen<sup>13</sup>, C. Lacasta<sup>49</sup>, C. Lambropoulos<sup>9</sup>, J.W. Lamsa<sup>1</sup>, L. Lancieri<sup>47</sup>,  
 V. Lapin<sup>43</sup>, J-P. Laugier<sup>39</sup>, R. Lauhakangas<sup>13</sup>, G. Leder<sup>50</sup>, F. Ledroit<sup>12</sup>, R. Leitner<sup>29</sup>, Y. Lemoigne<sup>39</sup>, J. Lemonne<sup>2</sup>,  
 G. Lenzen<sup>52</sup>, V. Lepeltier<sup>18</sup>, T. Lesiak<sup>16</sup>, J.M. Levy<sup>8</sup>, E. Lieb<sup>52</sup>, D. Liko<sup>50</sup>, J. Lindgren<sup>13</sup>, R. Lindner<sup>52</sup>,  
 A. Lipniacka<sup>51</sup>, I. Lippi<sup>35</sup>, B. Loerstad<sup>23</sup>, M. Lokajicek<sup>10</sup>, J.G. Loken<sup>34</sup>, A. Lopez-Fernandez<sup>7</sup>, M.A. Lopez Aguera<sup>42</sup>,  
 M. Los<sup>30</sup>, D. Loukas<sup>9</sup>, J.J. Lozano<sup>49</sup>, P. Lutz<sup>6</sup>, L. Lyons<sup>34</sup>, G. Maehlum<sup>32</sup>, J. Maillard<sup>6</sup>, A. Maio<sup>20</sup>, A. Maltezos<sup>9</sup>,  
 F. Mandl<sup>50</sup>, J. Marco<sup>42</sup>, M. Margoni<sup>35</sup>, J-C. Marin<sup>7</sup>, A. Markou<sup>9</sup>, T. Maron<sup>52</sup>, S. Marti<sup>49</sup>, F. Matorras<sup>42</sup>,  
 C. Matteuzzi<sup>27</sup>, G. Matthiae<sup>38</sup>, M. Mazzucato<sup>35</sup>, M. Mc Cubbin<sup>21</sup>, R. Mc Kay<sup>1</sup>, R. Mc Nulty<sup>21</sup>, G. Meola<sup>11</sup>,  
 C. Meroni<sup>27</sup>, W.T. Meyer<sup>1</sup>, M. Michelotto<sup>35</sup>, I. Mikulec<sup>50</sup>, L. Mirabito<sup>24</sup>, W.A. Mitaroff<sup>50</sup>, G.V. Mitselmakher<sup>14</sup>,  
 U. Mjoernmark<sup>23</sup>, T. Moa<sup>45</sup>, R. Moeller<sup>28</sup>, K. Moenig<sup>7</sup>, M.R. Monge<sup>11</sup>, P. Morettini<sup>11</sup>, H. Mueller<sup>15</sup>, W.J. Murray<sup>37</sup>,  
 B. Muryn<sup>16</sup>, G. Myatt<sup>34</sup>, F.L. Navarria<sup>5</sup>, P. Negri<sup>27</sup>, R. Nicolaidou<sup>3</sup>, B.S. Nielsen<sup>28</sup>, B. Nijhar<sup>21</sup>, V. Nikolaenko<sup>43</sup>,  
 P.E.S. Nilsen<sup>4</sup>, P. Niss<sup>45</sup>, A. Nomerotski<sup>35</sup>, V. Obraztsov<sup>43</sup>, A.G. Olshevski<sup>14</sup>, R. Orava<sup>13</sup>, A. Ostankov<sup>43</sup>,  
 K. Osterberg<sup>13</sup>, A. Ouraou<sup>39</sup>, M. Paganoni<sup>27</sup>, R. Pain<sup>22</sup>, H. Palka<sup>16</sup>, Th.D. Papadopoulou<sup>31</sup>, L. Pape<sup>7</sup>, F. Parodi<sup>11</sup>,  
 A. Passeri<sup>41</sup>, M. Pegoraro<sup>35</sup>, J. Pennanen<sup>13</sup>, L. Peralta<sup>20</sup>, V. Perevozchikov<sup>43</sup>, H. Pernegger<sup>50</sup>, M. Pernicka<sup>50</sup>,  
 A. Perrotta<sup>5</sup>, C. Petridou<sup>47</sup>, A. Petrolini<sup>11</sup>, L. Petrovich<sup>43</sup>, F. Pierre<sup>39</sup>, M. Pimenta<sup>20</sup>, O. Pingot<sup>2</sup>, S. Plaszczynski<sup>18</sup>,  
 O. Podobrin<sup>15</sup>, M.E. Pol<sup>17</sup>, G. Polok<sup>16</sup>, P. Poropat<sup>47</sup>, V. Pozdniakov<sup>14</sup>, P. Privitera<sup>15</sup>, A. Pullia<sup>27</sup>, D. Radojicic<sup>34</sup>,  
 S. Ragazzi<sup>27</sup>, H. Rahmani<sup>31</sup>, P.N. Ratoff<sup>19</sup>, A.L. Read<sup>32</sup>, P. Rebecchi<sup>7</sup>, N.G. Redaelli<sup>27</sup>, M. Regler<sup>50</sup>, D. Reid<sup>7</sup>,  
 P.B. Renton<sup>34</sup>, L.K. Resvanis<sup>3</sup>, F. Richard<sup>18</sup>, M. Richardson<sup>21</sup>, J. Ridky<sup>10</sup>, G. Rinaudo<sup>46</sup>, I. Roditi<sup>17</sup>, A. Romero<sup>46</sup>,  
 I. Roncagliolo<sup>11</sup>, P. Ronchese<sup>35</sup>, C. Ronnqvist<sup>13</sup>, E.I. Rosenberg<sup>1</sup>, S. Rossi<sup>7</sup>, E. Rosso<sup>7</sup>, P. Roudeau<sup>18</sup>, T. Rovelli<sup>5</sup>,  
 W. Ruckstuhl<sup>30</sup>, V. Ruhlmann-Kleider<sup>39</sup>, A. Ruiz<sup>42</sup>, K. Rybicki<sup>16</sup>, H. Saarikko<sup>13</sup>, Y. Sacquin<sup>39</sup>, G. Sajot<sup>12</sup>, J. Salt<sup>49</sup>,  
 J. Sanchez<sup>25</sup>, M. Sannino<sup>11,40</sup>, S. Schael<sup>7</sup>, H. Schneider<sup>15</sup>, M.A.E. Schyns<sup>52</sup>, G. Sciolla<sup>46</sup>, F. Scuri<sup>47</sup>, A.M. Segar<sup>34</sup>,  
 A. Seitz<sup>15</sup>, R. Sekulin<sup>37</sup>, M. Sessa<sup>47</sup>, G. Sette<sup>11</sup>, R. Seufert<sup>15</sup>, R.C. Shellard<sup>36</sup>, I. Siccama<sup>30</sup>, P. Siegrist<sup>39</sup>

S.Simonetti<sup>11</sup>, F.Simonetto<sup>35</sup>, A.N.Sjsakian<sup>14</sup>, G.Skjevling<sup>32</sup>, G.Smadja<sup>39,24</sup>, O.Smirnova<sup>14</sup>, G.R.Smith<sup>37</sup>, R.Sosnowski<sup>51</sup>, D.Souza-Santos<sup>36</sup>, T.S.Spasooff<sup>12</sup>, E.Spiriti<sup>41</sup>, S.Squarcia<sup>11</sup>, H.Staek<sup>52</sup>, C.Stanescu<sup>41</sup>, S.Stapnes<sup>32</sup>, G.Stavropoulos<sup>9</sup>, F.Stichelbaut<sup>2</sup>, A.Stocchi<sup>18</sup>, J.Strauss<sup>50</sup>, J.Straver<sup>7</sup>, R.Strub<sup>8</sup>, B.Stugu<sup>4</sup>, M.Szczekowski<sup>7</sup>, M.Szeptycka<sup>51</sup>, P.Szymanski<sup>51</sup>, T.Tabarelli<sup>27</sup>, O.Tchikilev<sup>43</sup>, G.E.Theodosiou<sup>9</sup>, A.Tilquin<sup>26</sup>, J.Timmermans<sup>30</sup>, V.G.Timofeev<sup>14</sup>, L.G.Tkatchev<sup>14</sup>, T.Todorov<sup>8</sup>, D.Z.Toet<sup>30</sup>, O.Toker<sup>13</sup>, B.Tome<sup>20</sup>, E.Torassa<sup>46</sup>, L.Tortora<sup>41</sup>, D.Treille<sup>7</sup>, U.Trevisan<sup>11</sup>, W.Trischuk<sup>7</sup>, G.Tristram<sup>6</sup>, C.Troncon<sup>27</sup>, A.Tsirou<sup>7</sup>, E.N.Tsyganov<sup>14</sup>, M.Turala<sup>16</sup>, M-L.Turluer<sup>39</sup>, T.Tuuva<sup>13</sup>, I.A.Tyapkin<sup>22</sup>, M.Tyndel<sup>37</sup>, S.Tzamaris<sup>21</sup>, S.Ueberschaer<sup>52</sup>, O.Ullaland<sup>7</sup>, V.Uvarov<sup>43</sup>, G.Valenti<sup>5</sup>, E.Vallazza<sup>46</sup>, J.A.Valls Ferrer<sup>49</sup>, C.Vander Velde<sup>2</sup>, G.W.Van Apeldoorn<sup>30</sup>, P.Van Dam<sup>30</sup>, M.Van Der Heijden<sup>30</sup>, W.K.Van Doninck<sup>2</sup>, P.Vaz<sup>7</sup>, G.Vegni<sup>27</sup>, L.Ventura<sup>35</sup>, W.Venus<sup>37</sup>, F.Verbeure<sup>2</sup>, M.Verlato<sup>35</sup>, L.S.Vertogradov<sup>14</sup>, D.Vilanova<sup>39</sup>, P.Vincent<sup>24</sup>, L.Vitale<sup>13</sup>, E.Vlasov<sup>43</sup>, A.S.Vodopyanov<sup>14</sup>, M.Vollmer<sup>52</sup>, M.Voutilainen<sup>13</sup>, V.Vrba<sup>41</sup>, H.Wahlen<sup>52</sup>, C.Walck<sup>45</sup>, F.Waldner<sup>47</sup>, A.Wehr<sup>52</sup>, M.Weierstall<sup>52</sup>, P.Weilhammer<sup>7</sup>, J.Werner<sup>52</sup>, A.M.Wetherell<sup>7</sup>, J.H.Wickens<sup>2</sup>, G.R.Wilkinson<sup>34</sup>, W.S.C.Williams<sup>34</sup>, M.Winter<sup>8</sup>, M.Witek<sup>16</sup>, G.Wormser<sup>18</sup>, K.Woschnagg<sup>48</sup>, N.Yamdagni<sup>45</sup>, P.Yepes<sup>7</sup>, A.Zaitsev<sup>43</sup>, A.Zalewska<sup>16</sup>, P.Zalewski<sup>18</sup>, D.Zavrtanik<sup>44</sup>, E.Zevgolatakos<sup>9</sup>, G.Zhang<sup>52</sup>, N.I.Zimin<sup>14</sup>, M.Zito<sup>39</sup>, R.Zuberi<sup>34</sup>, R.Zukanovich Funchal<sup>6</sup>, G.Zumerle<sup>35</sup>, J.Zuniga<sup>49</sup>

<sup>1</sup> Ames Laboratory and Department of Physics, Iowa State University, Ames IA 50011, USA

<sup>2</sup> Physics Department, Univ. Instelling Antwerpen, Universiteitsplein 1, B-2610 Wilrijk, Belgium and IIHE, ULB-VUB, Pleinlaan 2, B-1050 Brussels, Belgium

<sup>3</sup> and Faculté des Sciences, Univ. de l'Etat Mons, Av. Maistriau 19, B-7000 Mons, Belgium

<sup>4</sup> Physics Laboratory, University of Athens, Solonos Str. 104, GR-10680 Athens, Greece

<sup>5</sup> Department of Physics, University of Bergen, Allégaten 55, N-5007 Bergen, Norway

<sup>6</sup> Dipartimento di Fisica, Università di Bologna and INFN, Via Irnerio 46, I-40126 Bologna, Italy

<sup>7</sup> Collège de France, Lab. de Physique Corpusculaire, IN2P3-CNRS, F-75231 Paris Cedex 05, France

<sup>8</sup> CERN, CH-1211 Geneva 23, Switzerland

<sup>9</sup> Centre de Recherche Nucléaire, IN2P3 - CNRS/ULP - BP20, F-67037 Strasbourg Cedex, France

<sup>10</sup> Institute of Nuclear Physics, N.C.S.R. Demokritos, P.O. Box 60228, GR-15310 Athens, Greece

<sup>11</sup> FZU, Inst. of Physics of the C.A.S. High Energy Physics Division, Na Slovance 2, CS-180 40, Praha 8, Czechoslovakia

<sup>12</sup> Dipartimento di Fisica, Università di Genova and INFN, Via Dodecaneso 33, I-16146 Genova, Italy

<sup>13</sup> Institut des Sciences Nucléaires, IN2P3-CNRS, Université de Grenoble 1, F-38026 Grenoble, France

<sup>14</sup> Research Institute for High Energy Physics, SEFT, Siltavuorenpenger 20 C, SF-00170 Helsinki, Finland

<sup>15</sup> Joint Institute for Nuclear Research, Dubna, Head Post Office, P.O. Box 79, 101 000 Moscow, Russian Federation

<sup>16</sup> Institut für Experimentelle Kernphysik, Universität Karlsruhe, Postfach 6980, D-7500 Karlsruhe 1, Germany

<sup>17</sup> High Energy Physics Laboratory, Institute of Nuclear Physics, Ul. Kawiora 26 a, PL-30055 Krakow 30, Poland

<sup>18</sup> Centro Brasileiro de Pesquisas Físicas, rua Xavier Sigaud 150, RJ-22290 Rio de Janeiro, Brazil

<sup>19</sup> Université de Paris-Sud, Lab. de l'Accélérateur Linéaire, IN2P3-CNRS, Bat 200, F-91405 Orsay, France

<sup>20</sup> School of Physics and Materials, University of Lancaster, GB - Lancaster LA1 4YB, UK

<sup>21</sup> LIP, IST, FCUL - Av. Elias Garcia, 14 - 1º, P-1000 Lisboa Codex, Portugal

<sup>22</sup> Department of Physics, University of Liverpool, P.O. Box 147, GB - Liverpool L69 3BX, UK

<sup>23</sup> LPNHE, IN2P3-CNRS, Universités Paris VI et VII, Tour 33 (RdC), 4 place Jussieu, F-75252 Paris Cedex 05, France

<sup>24</sup> Department of Physics, University of Lund, Sölvegatan 14, S-22363 Lund, Sweden

<sup>25</sup> Université Claude Bernard de Lyon, IPNL, IN2P3-CNRS, F-69622 Villeurbanne Cedex, France

<sup>26</sup> Universidad Complutense, Avda. Complutense s/n, E-28040 Madrid, Spain

<sup>27</sup> Univ. d'Aix - Marseille II - CPP, IN2P3-CNRS, F-13288 Marseille Cedex 09, France

<sup>28</sup> Dipartimento di Fisica, Università di Milano and INFN, Via Celoria 16, I-20133 Milan, Italy

<sup>29</sup> Niels Bohr Institute, Blegdamsvej 17, DK-2100 Copenhagen 0, Denmark

<sup>30</sup> NC, Nuclear Centre of MFF, Charles University, Areal MFF, V Holesovickach 2, CS-180 00, Praha 8, Czechoslovakia

<sup>31</sup> NIKHEF-H, Postbus 41882, NL-1009 DB Amsterdam, The Netherlands

<sup>32</sup> National Technical University, Physics Department, Zografou Campus, GR-15773 Athens, Greece

<sup>33</sup> Physics Department, University of Oslo, Blindern, N-1000 Oslo 3, Norway

<sup>34</sup> Dpto. Fisica, Univ. Oviedo, C/P.Jimenez Casas, S/N-33006 Oviedo, Spain

<sup>35</sup> Department of Physics, University of Oxford, Keble Road, Oxford OX1 3RH, UK

<sup>36</sup> Dipartimento di Fisica, Università di Padova and INFN, Via Marzolo 8, I-35131 Padua, Italy

<sup>37</sup> Depto. de Fisica, Pontificia Univ. Católica, C.P. 38071 RJ-22453 Rio de Janeiro, Brazil

<sup>38</sup> Rutherford Appleton Laboratory, Chilton, GB - Didcot OX11 0QX, UK

<sup>39</sup> Dipartimento di Fisica, Università di Roma II and INFN, Tor Vergata, I-00173 Rome, Italy

<sup>40</sup> Centre d'Etude de Saclay, DSM/DAPNIA, F-91191 Gif-sur-Yvette Cedex, France

<sup>41</sup> Dipartimento di Fisica-Università di Salerno, I-84100 Salerno, Italy

<sup>42</sup> Istituto Superiore di Sanità, Ist. Naz. di Fisica Nucl. (INFN), Viale Regina Elena 299, I-00161 Rome, Italy

<sup>43</sup> C.E.A.F.M., C.S.I.C. - Univ. Cantabria, Avda. los Castros, S/N-39006 Santander, Spain

<sup>44</sup> Inst. for High Energy Physics, Serpukov P.O. Box 35, Protvino, (Moscow Region), Russian Federation

<sup>45</sup> J. Stefan Institute and Department of Physics, University of Ljubljana, Jamova 39, SI-61000 Ljubljana, Slovenia

<sup>46</sup> Fysikum, Stockholm University, Box 6730, S-113 85 Stockholm, Sweden

<sup>47</sup> Dipartimento di Fisica Sperimentale, Università di Torino and INFN, Via P. Giuria 1, I-10125 Turin, Italy

<sup>48</sup> Dipartimento di Fisica, Università di Trieste and INFN, Via A. Valerio 2, I-34127 Trieste, Italy

<sup>49</sup> and Istituto di Fisica, Università di Udine, I-33100 Udine, Italy

<sup>50</sup> Department of Radiation Sciences, University of Uppsala, P.O. Box 535, S-751 21 Uppsala, Sweden

<sup>51</sup> IFIC, Valencia-CSIC, and D.F.A.M.N., U. de Valencia, Avda. Dr. Moliner 50, E-46100 Burjassot (Valencia), Spain

<sup>52</sup> Institut für Hochenergiephysik, Österr. Akad. d. Wissensch., Nikolsdorfergasse 18, A-1050 Vienna, Austria

<sup>53</sup> Inst. Nuclear Studies and University of Warsaw, Ul. Hoza 69, PL-00681 Warsaw, Poland

<sup>54</sup> Fachbereich Physik, University of Wuppertal, Postfach 100 127, D-5600 Wuppertal 1, Germany

# 1 Introduction

This letter describes a study of events consisting of a lepton pair and one pair of charged particles, recorded in the DELPHI detector at LEP. The lepton pair,  $\ell^+\ell^-$ , may be  $e^+e^-$ ,  $\mu^+\mu^-$  or  $\tau^+\tau^-$ . The other pair of particles, hereafter called V, can be either a lepton pair or a hadron pair. Events of this type can be produced through second order QED processes, when an off-mass-shell photon from initial or final state bremsstrahlung materializes into a pair of fermions. Calculations of rates and differential distributions have been made in reference [1]. These simple final states are of interest for several reasons. They allow one to extend the precision tests of QED from the final states with a real photon radiated to the case where a virtual photon is produced. Also, although they are rather rare, they can be a significant background in searches for the Higgs bosons[2]. Finally, an anomaly in the production rate or distribution of events could be a signal of new physics beyond the standard model. A possible small excess in the  $e^+e^-\mu^+\mu^-$  channel was suggested in 1990 by the AMY collaboration[3], working in the TRISTAN/KEK accelerator, and later the ALEPH collaboration[4] reported an excess of  $\tau^+\tau^-V$  events. In July 1991 the MarkII[5] collaboration using data taken at PEP/SLAC and the OPAL[6] and the DELPHI[7] collaborations using data from LEP/CERN all quoted no discrepancies with the standard model. More recently, the AMY collaboration reported that with the increase in statistics, their data are not significantly different from expectations[8].

The data analyzed here were recorded by DELPHI during 1990 and 1991 in a sample corresponding to 365,000 hadronic  $Z^0$  decays. The events were taken at centre of mass energies between 88.2 and 94.2 GeV with 74% at the peak of the  $Z^0$  cross section; the integrated luminosity was  $15.7 \text{ pb}^{-1}$ .

The organization of the paper is the following: in section 2 a description of the essential features of the DELPHI detector is given. In section 3, the Monte-Carlo simulation is presented. The event selection is explained in detail in section 4 and the event identification is described in section 5. In section 6, the results are given, and in section 7 a check with  $ll\gamma$  events is presented. Finally conclusions are drawn in section 8.

## 2 Apparatus

An exhaustive description of the DELPHI detector can be found elsewhere [9]. The specific properties relevant to this analysis are now described.

Charged particle tracks are measured in the 1.2 Tesla magnetic field by three cylindrical tracking chambers: the Inner Detector (ID) covers polar angles from  $30^\circ$  to  $150^\circ$  at radii 12 to 28 cm, the Time Projection Chamber (TPC), the main tracking device, covers polar angles from  $20^\circ$  to  $160^\circ$  and radii between 35 and 111 cm and the Outer Detector (OD) covers polar angles from  $43^\circ$  to  $137^\circ$  at radii between 198 and 206 cm.

The Microvertex Detector (VD) consists of three independent half-shells inserted between the beam pipe and the ID. Each half-shell contains concentric layers of microstrip detectors located at radii 6.3 (only for 1991 data), 9 and 11 cm. They measure the transverse coordinates and cover polar angles from  $43^\circ$  to  $137^\circ$ . It was used in the analysis after the event selection to check on possible photon conversions occurring between the VD and the TPC sensitive regions.

The electromagnetic energy is measured by the High Density Projection Chamber (HPC) in the barrel and by the Forward Electromagnetic Calorimeter (FEMC). The HPC has nine layers of lead and gas covering polar angles from  $43^\circ$  to  $137^\circ$  and radii

between 208 and 260 cm. The FEMC has lead glass blocks covering polar angles from  $10^\circ$  to  $36^\circ$  and from  $144^\circ$  to  $170^\circ$ .

Hadron shower energies are measured by combining the measurements from the Hadron Calorimeter (the instrumented iron return yoke for the magnet), covering polar angles from  $10^\circ$  to  $170^\circ$ , and the electromagnetic calorimeter.

Muons are identified by their penetration through the yoke to the Muon Barrel (MUB) and Forward (MUF) chambers, which have layers embedded in and outside the iron yoke, and cover polar angles from  $9^\circ$  to  $43^\circ$ , from  $52^\circ$  to  $128^\circ$  and from  $137^\circ$  to  $171^\circ$ . The calorimeters also distinguish hadron or electromagnetic showers from minimum ionizing particles.

The Small Angle Tagger (SAT) was used to measure the luminosity. It consists of an electromagnetic calorimeter covering polar angles from 43 to 135 mrad.

### 3 The simulation of known physics processes

At the  $Z^0$  pole, the main processes contributing to the  $\ell^+\ell^-V$  signal are the  $Z^0$  decays into leptons and the t-channel photon exchange, both with virtual photon production providing the other pair of charged particles. There is a small contribution to the signal from multiperipheral and conversion-type diagrams[1].

The generation of the  $\ell^+\ell^-V$  events uses a Monte-Carlo program that is derived from the one described in reference [1], but with the  $Z^0$  diagrams added to the photon ones. The electromagnetic coupling constant is assumed equal to  $1/128$  for the  $Z^0$  propagator and  $1/137$  for the photon propagator. This generator program does not include initial radiation, hence the cross sections obtained were multiplied by a correction factor depending on the energy in the centre of mass (0.74 at the  $Z^0$  peak).

The program was modified to account for final states containing a pion pair. This was done by generating  $\ell^+\ell^-\mu^+\mu^-$  events, changing the muon pair in a pion pair, and then weighting each of them with a factor taken from the experimentally measured ratio R of  $\pi^+\pi^-$  production to  $\mu^+\mu^-$  production[10] in low energy  $e^+e^-$  annihilations. This factor, used up to a V mass of 1.6 GeV, takes into account both the resonant mass dependence around the  $\rho$  region and the different angular decay distributions for pion and muon pairs. Final states containing other hadron pairs have a contribution one order of magnitude smaller [11] and were not simulated.

A total of 500 events (about  $250 \text{ pb}^{-1}$ ) were generated for each final state, requesting pair invariant mass greater than  $50 \text{ MeV}/c^2$  and polar angle greater than  $15^\circ$  (except for the  $\tau^+\tau^-V$  channel). They were submitted to the full detector simulation[12] allowing for all decays and interactions, and the results were processed by the same reconstruction and analysis programs as the raw data from LEP.

In addition to the simulated  $\ell^+\ell^-V$  events, other sets of generated events were also passed through the detector simulation, reconstruction and analysis programs in order to estimate the background. The data samples used comprised  $20 \text{ pb}^{-1}$  of simulated Bhabha events ( $e^+e^- \rightarrow e^+e^-(\gamma)$ ) from the program BABAMC[13],  $35 \text{ pb}^{-1}$  of simulated Muon events ( $e^+e^- \rightarrow \mu^+\mu^-(\gamma)$ ) from DYMU3[14],  $50 \text{ pb}^{-1}$  of simulated Tau events ( $e^+e^- \rightarrow \tau^+\tau^-(\gamma)$ ) from KORALZ[15] and  $25 \text{ pb}^{-1}$  of simulated hadronic events ( $e^+e^- \rightarrow q\bar{q}(\gamma)$ ) from JETSET7.3[16].

## 4 Event selection

The charged particle multiplicity distinguishes  $\ell^+\ell^-V$  events from most dilepton and hadronic final states. Candidate events are required to have four charged particles or, to accept  $\tau^+\tau^-V$  events in which one of the  $\tau$  decays into 3 charged pions, six charged particles. Background events come from  $\tau^+\tau^-$  events with 3-prong decay of one or both of the  $\tau$ 's,  $\ell^+\ell^-\gamma$  events where the photon converts, and hadronic jets at small angles to the beam, where the efficiency for reconstructing particles is low. In order to reduce these backgrounds, the characteristic topology of  $\ell^+\ell^-V$  events is exploited, favoring a quasi 3-body configuration, and with a wide range in the invariant mass of the  $\ell V$  system (constrained in the  $\tau^+\tau^-$  events) or of the  $V$  pair (peaked at very low masses in the contribution from real photon conversions).

In the following subsections the successive selection criteria will be described in detail.

### 4.1 Selection of charged particles

Charged particles must come from the interaction region within 6 cm along the beam direction and within 3 cm in the transverse plane (4 cm for polar angles lower than  $40^\circ$  or greater than  $140^\circ$ ). They should have a polar angle between  $25^\circ$  and  $155^\circ$ , and momentum greater than 0.2 GeV/c. Events must have four or six charged particles and balance charge. If there were only four charged particles, up to two additional charged particles not coming from the interaction region were allowed; these may be the result of an associated photon conversion. To remove photon-photon interactions the sum of the absolute momenta of the charged particles must be above 15 GeV (see figure 1) and there must be at least two jets. The jet topology was determined using the jet cluster algorithm JADE[16] with default parameter  $y_{\text{cut}} = 0.05$ .

At this first level about 4100 events were kept.

### 4.2 Suppression of $\tau^+\tau^-$ background

The background from  $\tau^+\tau^-$  events can be much reduced by applying a cut on the lowest invariant mass of all possible triplets of particles: in a perfectly reconstructed tau decay, this mass should not exceed 1.7 GeV, while for the signal no such constraint is present. For the sample with four charged particles a minimal mass of 2.5 GeV/c<sup>2</sup> was imposed on all combinations of three charged particles. For the sample with six charged particles, all possible combinations of three charged particles with total charge  $\pm 1$  and invariant mass lower than 1.7 GeV/c<sup>2</sup> were counted. Events with one and only one such combination (a  $\tau$  decay candidate) and an invariant mass of the other three particles greater than 2.5 GeV/c<sup>2</sup> were retained. The particles composing the accepted combination were substituted by the vector sum of their momenta, reducing this case to four charged particles.

Figure 2 shows that the triplet mass spectrum is dominated up to 1.6 GeV/c<sup>2</sup> by the  $\tau$  into  $3\pi$  contribution. The reliability of the Monte Carlo simulation of the  $3\pi$  mass distribution was verified using selected decays of the  $Z^0$  into  $\tau^+\tau^-$ [17]. It can be seen that the 2.5 GeV/c<sup>2</sup> cut removes most of this background; the contamination remaining in the final sample was estimated to be  $1.6 \pm 0.5$  events. This contribution comes from events in which one of the charged pions has suffered a nuclear interaction in the material between the decay vertex and the TPC, resulting in a badly reconstructed  $\tau$  mass. Above

1.6 GeV/c<sup>2</sup>, the excess above the expected  $\ell^+\ell^-V$  signal is mainly due to the background from hadronic events and leptonic events with converted photons.

After the mass selection 316 events remained.

### 4.3 Rejection of converted photons

Photon conversions are recognized since they give two charged particle tracks which have almost the same polar angle and very small invariant mass. In the transverse plane the circular trajectories of the two tracks are almost tangent. Therefore, for every pair of particles, the transverse trajectories were extrapolated to the point where the tangents were parallel and the distance between them was smallest. The pair was considered a converted photon if at that point the invariant mass was below 85 MeV/c<sup>2</sup> and the distance between the trajectories was less than 4.5 cm. For particles with momentum lower than 0.6 GeV/c, the cut was increased to take into account multiple scattering effects. For the sample with six charged particles, the three particles making the  $\tau$  candidate were not used. In figure 3 the invariant mass of the pair is shown, comparing data and signal Monte-Carlo simulation (multiplied by 100). No events from the Bhabha and Muon Monte-Carlo simulated samples survive this selection.

These cuts removed 246 events and thus 70 candidate events remained.

### 4.4 Removal of hadronic background

The preferred topologies of  $\ell^+\ell^-V$  events are 1-3 (i.e. 2 jets with the V and one lepton in the same jet) and 1-1-2 (i.e. 3 jets with the V in a separate jet), while hadronic background due to lost tracks often have 2-2 and 1-3 configurations. Hadronic events in 1-3 topology are highly suppressed by the previous triplet mass cut. The events with 2-2 topology were rejected. With this cut 39 of the 2-2 type events were removed from the 70 candidate events. This criterion is stable for variations of up to  $\pm 0.03$  in the  $y_{\text{cut}}$  parameter.

The 39 events removed had more extra-tracks, that is tracks not extrapolating to the interaction region, and very few identified leptons; indeed, only 6 out of the 31 remaining candidates had extra tracks, while 23 out of the 39 2-2 events had at least one extra track, and only 4 out of the 39 2-2 events had an identified lepton (3 candidate muons with momentum greater than 5 GeV/c, and 1 candidate electron with energy greater than 5 GeV/c). These results confirm that the rejected sample mostly contained  $q\bar{q}$  events.

The quasi 3-body configuration of the  $\ell^+\ell^-V$  events was used as a further selection, to eliminate hadronic events with undetected particles. After merging the two particles that make the V into a single particle, the resulting configuration should be planar, even for  $\tau^+\tau^-V$  events, since in this case the charged decay products follow closely the direction of the tau. Therefore the sum of its three internal angles should be approximately 360°. Rejecting the events for which there is no combination of two oppositely charged particles for the V giving a sum of angles greater than 357°, 2 out of the 31 candidates were removed. The efficiency of this cut is high for the signal: 99% for the  $e^+e^-V$  and  $\mu^+\mu^-V$  events and 85% for the  $\tau^+\tau^-V$  events.

Finally, in hadronic events, large amounts of hadronic energy not associated to charged particles can be expected, due to neutral particles and charged particles lost in the forward region, while for the  $\ell^+\ell^-V$  events this is not the case: 99% of the simulated  $e^+e^-V$  and  $\mu^+\mu^-V$  events and 95% of the simulated  $\tau^+\tau^-V$  events deposit less than 10 GeV in the

hadronic calorimeter unassociated to charged particles. Therefore 2 candidates which had deposits of unassociated hadronic energy greater than 10 GeV were removed.

After all the selections, 27 candidate events were retained, which constituted the final sample.

Applying this analysis to the simulated  $q\bar{q}$  background sample,  $1.8 \pm 1.0$  events survive the cuts.

However, as the  $q\bar{q}$  Monte-Carlo programs are not well tested in the low charged multiplicity domain, an estimate of the hadronic background was made from the data. In this estimation the events with unbalanced charge were used, since the incomplete hadronic events are not necessarily balanced in charge. In fact, before the topology cut, where the other main backgrounds were already highly suppressed, 39 balanced charge events and 32 unbalanced charge events were found with topology 2-2. Removing the charge conservation cut, 2 unbalanced charge events surviving all the other cuts were found. However, after inspection, one of these two events was identified as a  $\ell^+\ell^-V$  event where there was a wrong charge identification in one of the tracks (0.7 events are expected from the  $\ell\ell V$  Monte-Carlo). Therefore, according to the ratio of the hadronic samples in the balanced and unbalanced charge events, the remaining hadronic background in the candidate sample is estimated to be  $1.2 \pm 1.2$  events.

This is in good agreement with the above Monte Carlo estimate; taking the weighted average one gets  $1.6 \pm 0.8$  events.

## 5 Identification of events

The 27 candidate events were classified as  $\tau^+\tau^-V$ ,  $e^+e^-V$  or  $\mu^+\mu^-V$ , according to the multiplicity, the total measured energy, and the lepton identification.

To define the V, each pair of oppositely charged particles was merged into a single one. If the resulting 3-particle configuration had the sum of its three internal angles higher than  $357^\circ$ , the pair was chosen as the V candidate. When more than one such pair existed, and if the two particles composing the V were not identified as leptons of different flavour, the one with the lowest mass was taken.

### 5.1 Identification of $\tau^+\tau^-V$ events

Events with 6 charged particles, or events with 4 charged particles and sum of their absolute momenta lower than 65 GeV/c and total electromagnetic energy below 65 GeV, were considered  $\tau^+\tau^-V$  events. This cut retains 86% of the simulated  $\tau^+\tau^-V$  events, while the contamination from simulated  $e^+e^-V$  or  $\mu^+\mu^-V$  events is 1%. There were 7 events classified as  $\tau^+\tau^-V$ .

All events but one contained at least one identified electron or muon, a condition which was not imposed on the selection and which confirms that the candidate events are not significantly dominated by hadronic background. The spread in mass of the lowest mass triplet of charged particle tracks and the fact that at least one particle of this triplet was identified as a lepton in 5 out of the 7  $\tau^+\tau^-V$  events, also excludes any significant contamination due to poorly reconstructed  $\tau^+\tau^-$  decaying into  $3\pi$ . The total background to this channel is estimated, as described in the previous sections, to be  $1.6 \pm 0.5$  events from  $\tau^+\tau^-$  background and  $1.6 \pm 0.8$  events from hadronic background.



## 5.2 Identification of $e^+e^-V$ and $\mu^+\mu^-V$ events

The remaining 20 events were classified as  $e^+e^-V$  or  $\mu^+\mu^-V$  events.

Out of these 20 events, 11 events were identified as  $e^+e^-V$  by demanding that one of the leptons (not making the  $V$ ) had  $E_{em}/p$  between 0.6 and 1.7, where  $E_{em}$  was the energy measured in the electromagnetic calorimeter and  $p$  the measured momentum.

Of the remaining 9 events, 7 had hits in the muon chambers associated to one of the charged particles not making the  $V$ , and were classified as  $\mu\mu V$  events. Of the other 2 events, one had both leptons with  $E_{em}/p$  below 0.1 and  $E_{had}/p$  below 0.1 ( $E_{had}$  is the energy measured in the hadronic calorimeter associated to the particle) and so was also classified as  $\mu\mu V$  event. The other event had one lepton with  $E_{had}/p$  below 0.1 and  $E_{em}/p = 5.9$  and the other lepton with  $E_{had}/p$  and  $E_{em}/p$  below 0.1. It was assumed to be a  $\mu\mu\gamma V$  event where the radiated photon was collinear with one of the muons.

## 5.3 Classification of the $V$

If a particle making the  $V$  was energetic, it was classified using the electromagnetic calorimeter and muon chambers information. Lower energy particles were identified using the energy per unit track-length deposited in the gas of the TPC ( $dE/dx$ ).

In all candidate events except one, at least one of the particles of the  $V$  was successfully identified (with some ambiguity between muons and pions for low momentum particles) and the  $V$  was compatible with being a particle-antiparticle pair.

The information from the Microvertex Detector was used to confirm that photon conversions were properly eliminated by the cuts described in section 4.3. Of the 8  $V$ 's with mass below  $0.4 \text{ GeV}/c^2$  falling within the acceptance of the VD, 7 had associated hits in it, whereas most of the conversions should take place after this detector.

## 6 Results

The properties of the 27 candidates are given in table I (Ia- for 1990 data, Ib- for 1991 data). The results of this analysis are summarized on tables II and III. Figure 4 shows the distribution of the centre of mass energy of the events, ECM. Figures 5 to 7, show the comparisons of invariant masses and  $V$  energy between the observed data and the expectations for the signal. The invariant mass of the pair  $\ell^+\ell^-$  (the leptons not making the  $V$ ),  $m_{\ell\bar{\ell}}$ , was calculated as the recoil mass from the  $V$ , for all events except the one with the  $V$  mass of  $17.5 \text{ GeV}/c^2$ . For this last case, a  $\chi^2$  4-Constraint kinematical fit of the four particles momenta (one being the tau candidate, i.e, the vector sum of three particles) was performed to improve the errors on the calculated masses (the values of the masses for the  $V$  or  $\ell^+\ell^-$  have not changed significantly from the previous methods).

Within the statistics there is a reasonable agreement between data and Monte-Carlo predictions. There are however small discrepancies with the expected behaviour. On figure 4, there is an indication of a spread in centre of mass energy of the  $\tau^+\tau^-V$  candidates. There is also a small peak of 3 low  $V$  mass events and an event with an unusually high  $V$  mass ( $17.47 \pm 0.17 \text{ GeV}/c^2$ ) in the  $\tau^+\tau^-V$  channel (figure 5-b)). The three events with a low  $V$  mass had a centre of mass energy out of the  $Z^0$  peak, and were characterized by a very energetic  $V$ .

The high  $V$  mass event is shown in figure 8. In this event the  $V$  is composed of two identified muons recoiling against a  $25.8 \pm 0.8 \text{ GeV}/c^2$  invariant mass  $\tau^+\tau^-$  system. The mass resolution for this event was calculated from a  $\chi^2$  4-constraint kinematical fit of the

4 particles momenta. The number of events with a  $V$  mass greater than  $10 \text{ GeV}/c^2$  and  $\ell^+\ell^-$  mass lower than  $40 \text{ GeV}/c^2$  predicted by the  $\ell^+\ell^-V$  Monte Carlo is  $0.013 \pm 0.013$ .

## 7 Checks on $\ell\ell\gamma$ events

Another test of universality in the three leptonic channels was done by studying the production of  $\ell\ell\gamma$  events. This is directly related to the search for heavy excited charged leptons decaying into two normal leptons plus a photon, an analysis already published by DELPHI[18]. This analysis also corresponds to a total of 365,000 hadronic events. The event selection requested two charged particles with polar angles between  $25^\circ$  and  $155^\circ$  plus a photon with energy above 2 GeV and with an isolation angle with respect to the nearest charged particle larger than  $30^\circ$ . Table IV gives the number of events selected for each channel together with the Monte Carlo expectations from standard  $Z^0$  decays; for this analysis the selection on the centre of mass energy that was used in reference[18] was removed.

Table V gives the result of a modified study in which the minimum isolation angle for the photon was reduced to  $15^\circ$ , therefore covering an angular region similar to that of the  $\ell\ell V$  analysis.

As can be seen in the tables, the number of events found is in agreement with the standard Monte Carlo predictions.

## 8 Summary and conclusion

A search for  $\ell^+\ell^-V$  events with the DELPHI detector was performed on a sample corresponding to 365,000 hadronic  $Z^0$  decays. The results indicate no anomalous behaviour in any of the three channels,  $e^+e^-V$ ,  $\mu^+\mu^-V$  and  $\tau^+\tau^-V$ .

The final sample shows a small excess in the low  $V$  mass region for the  $\tau^+\tau^-V$  channel, although of no strong statistical significance. An event was found with an unusually high  $V$  mass of  $17.47 \pm 0.17 \text{ GeV}/c^2$  composed of two identified muons, recoiling from a  $\tau^+\tau^-$  system with invariant mass of  $25.8 \pm 0.8 \text{ GeV}/c^2$ .

An independent test on universality of the three lepton channels on  $\ell^+\ell^-V$  events, shows a good agreement between data and expectations.

## Acknowledgements

We would like to thank R. Kleiss for helpful discussions and J. Hilgart for providing an improved version of the code for the  $\ell^+\ell^-V$  model. We are greatly indebted to our technical collaborators and to the funding agencies for their support in building and operating the DELPHI detector, and to the members of the CERN-SL Division for the excellent performance of the LEP collider.

**Caption for table I**

- $E_{cm}$ : Energy in the center of mass (GeV).  
 $E_{ch}$ : Total Energy of the charged particles (GeV).  
 $E_{tem}$ : Total Electromagnetic Energy (GeV).  
 $N_{ch}$ : Number of charged particles.  
 $\ell^+\ell^-$ : Identification of the main leptons.  
 $m_{\ell\bar{\ell}}$ : Invariant mass of the main leptons, calculated as the recoil mass to the  $V$  ( $\text{GeV}/c^2$ ).  
 $V$ : Identification of the components of the  $V$ .  
 $m_V$ : Mass of the  $V$  ( $\text{GeV}/c^2$ ).  
 $m(3\pi)$ : Lowest invariant mass of all combinations of three charged particles with total charge  $\pm 1$  ( $\text{GeV}/c^2$ ).  
 $\theta_{open}(\circ)$ : Opening angle of the  $V$  (degrees).  
 $\theta_V$ : Angle of the  $V$  with the closest lepton (degrees).

**Table I a) 1990**

List of events that pass the selection criteria described in the text.

Run	Event	$E_{cm}$	$E_{ch}$	$E_{tem}$	$N_{ch}$	$\ell^+\ell^-$	$m_{\ell\bar{\ell}}$	$V$	$m_V$	$E_V$	$m(3\pi)$	$\theta_{open}(\circ)$	$\theta_V(\circ)$
1	8370	91.28	92.8	0.85	4	$\mu\mu$	85.6	$\pi\pi, \mu\mu$	0.79	5.5	20.9	16.7	90.1
2	12993	91.28	68.0	8.18	4	$\mu\mu$	90.3	$ee$	0.15	0.9	6.9	22.5	78.2
3	13824	40	89.29	44.3	4	$\tau\tau$	89.7	$ee$	0.41	1.5	5.0	34.8	40.8
4	14549	9611	94.27	42.7	11.74	6	$\tau\tau$	$\mu\mu$	0.37	31.0	14.2	0.7	100.7
5	15563	5372	92.27	128.7	1.41	4	$\mu\mu$	$\mu\mu$	1.16	11.4	30.0	12.8	88.1

**Table I b) 1991**

List of events that pass the selection criteria described in the text.

Run	Event	$E_{cm}$	$E_{ch}$	$E_{tem}$	$N_{ch}$	$\ell^+\ell^-$	$m_{\ell\bar{\ell}}$	V	mv	$E_V$	$m(3\pi)$	$\theta_{open}(\circ)$	$\theta_V(\circ)$	
6	21325	1292	91.24	76.7	50.0	4	ee	81.4	$\mu\mu$	0.43	9.3	14.0	4.0	45.2
7	21582	5248	91.24	86.6	32.9	4	ee	78.3	?	0.78	12.1	4.3	8.6	11.7
8	21919	31790	91.24	94.4	6.60	4	$\mu\mu$	81.2	ee	0.27	9.4	25.2	3.6	78.4
9	21982	12186	91.24	37.0	22.5	4	$\tau\tau$	77.7	$\mu\mu$	2.04	12.7	7.0	22.3	21.9
10	22479	873	91.25	88.5	83.4	4	ee	85.3	$\mu\mu$	2.19	5.8	8.6	48.6	23.4
11	22851	3361	91.24	39.7	0.16	4	$\tau\tau$	48.7	$\pi\pi$	0.90	32.6	3.1	3.3	25.1
12	22935	1601	91.24	91.2	1.26	4	$\mu\mu$	67.0	$\pi\pi$	0.97	21.0	14.2	6.0	35.2
13	23545	1549	91.24	91.0	0.18	4	$\mu\mu$	88.4	$\mu\mu, \pi\pi$	1.21	2.8	11.5	57.1	58.4
14	24605	5263	91.23	86.8	84.8	4	ee	89.0	$\mu\mu, \pi\pi$	0.96	2.2	11.3	49.1	68.2
15	25788	19204	91.95	74.7	93.6	4	ee	90.0	$\mu\mu, \pi\pi$	0.63	2.0	11.6	33.2	73.9
16	25926	2824	92.96	92.0	14.0	4	$\mu\mu$	48.0	ee	0.14	34.1	38.5	0.5	92.3
17	26405	11096	91.97	57.4	91.0	4	ee	82.1	ee	0.11	9.3	12.9	1.4	46.4
18	26405	13313	91.97	73.5	90.6	4	ee	86.5	$\mu\mu$	0.95	5.3	19.1	28.3	86.2
19	26410	3068	91.21	82.1	29.7	4	$\mu\mu$	53.3	ee	0.15	30.0	6.1	1.7	16.6
20	27909	1619	91.20	72.1	41.2	4	$\mu\mu$	45.9	ee	2.83	34.1	5.1	23.6	38.9
21	28057	4020	91.20	59.8	78.0	4	ee	77.1	ee	2.66	13.1	18.0	34.1	49.0
22	28113	13298	93.70	24.3	17.5	4	$\tau\tau$	77.6	ee	0.22	14.8	4.8	1.9	45.8
23	28224	3997	92.95	78.2	72.7	4	ee	71.4	$\mu\mu$	1.50	19.1	5.0	10.3	12.5
24	28271	3370	89.50	62.6	3.20	6	$\tau\tau$	25.4	$\mu\mu$	17.47	42.5	37.5	77.8	135.1
25	28313	8208	91.16	75.1	82.6	4	ee	89.0	$\mu\mu, \pi\pi$	0.61	2.1	13.4	29.0	89.6
26	28651	36055	88.47	32.5	29.3	4	$\tau\tau$	65.1	ee	0.24	20.3	13.8	2.2	85.6
27	28736	8200	91.95	85.9	48.4	4	ee	39.0	$\mu\mu$	4.56	37.8	12.4	22.9	38.6

**Table II**

Observed numbers of events compared to the expected numbers of events;  $\ell^+\ell^-V$  is the expected signal,  $\ell^+\ell^-\gamma$  represents the added contribution from Bhabha and Muon background simulated samples,  $\tau^+\tau^-$  is the  $\tau^+\tau^-$  background sample and  $q\bar{q}$  is the hadronic background sample.

Channel	Data			Monte-Carlo Expectations			
	1990	1991	Total	Signal $\ell\ell V$	$\ell\ell\gamma$	$\tau\tau$	$q\bar{q}$
$\ell^+\ell^-$							
$e^+e^-$	0	11	11	$9.5 \pm 1.1$	0	0	0
$\mu^+\mu^-$	3	6	9	$9.3 \pm 0.9$	0	0	0
$\tau^+\tau^-$	2	5	7	$3.9 \pm 0.4$	0	$1.6 \pm 0.5$	$1.6 \pm 0.8$
Total	5	22	27	$22.7 \pm 1.4$	0	$1.6 \pm 0.5$	$1.6 \pm 0.8$

**Table III**

Distribution of the candidates according to the V classification, as described in the text.

$\ell^+\ell^-$	V=ee	V= $\mu\mu$	V= $\pi\pi$	V= $\mu\mu, \pi\pi$	V=?	Total
$e^+e^-$	2	5	0	3	1	11
$\mu^+\mu^-$	5	1	1	2	-	9
$\tau^+\tau^-$	3	3	1	-	-	7
Total	10	9	2	5	1	27

**Table IV**

Number of  $\ell\ell\gamma$  events found for each channel, and number of events expected from standard processes (photon isolation greater than angle  $30^\circ$ ).

Channel	Observed	Expected
$ee\gamma$	166	$169 \pm 13$
$\mu\mu\gamma$	123	$126 \pm 10$
$\tau\tau\gamma$	75	$72 \pm 6$

Table V

Number of  $ll\gamma$  events found when the minimum photon isolation angle  $\theta_\gamma$  is reduced to  $15^\circ$ , and number of events expected from standard processes.

Channel	$15^\circ < \theta_\gamma < 30^\circ$		$\theta_\gamma > 15^\circ$	
	Observed	Expected	Observed	Expected
$ee\gamma$	23	$24 \pm 3$	189	$193 \pm 15$
$\mu\mu\gamma$	29	$18 \pm 2$	152	$144 \pm 11$
$\tau\tau\gamma$	10	$11 \pm 1.5$	85	$83 \pm 7$

## References

- [1] F.A. Berends, P. Daverveldt and R. Kleiss, Nucl. Phys. B **253** (1985) 421 and Comp. Phys. Comm. 40 (1986) 271., and P.Daverveldt, *Monte Carlo Simulation of Two Photon Processes*, Ph.D. Thesis, Rijksuniversiteit te Leiden, September, 1985.
- [2] DELPHI Collaboration, P.Abreu et al., Nucl. Phys. B **373** (1992) 3.
- [3] AMY Collaboration, Y.H.Ho et al., Phys. Lett. B **244** (1990) 573.
- [4] ALEPH Collaboration, D. Decamp et al., Phys. Lett. **263** B (1991) 112.
- [5] MARK II Collaboration, T.Barklow et al., Phys. Rev. Lett. **68** (1992) 13.
- [6] OPAL Collaboration, P.D.Acton et al., Phys. Lett. B **287** (1992) 389.
- [7] M.Pimenta, DELPHI Collaboration, *published in the Proceed. Joint Int'l Lepton-Photon Symposium & Europhysics Conference on High Energy Physics, Geneva, July '91, Vol.1, p.379.*
- [8] AMY Collaboration, KEK Preprint 92-36, AMY 92-1, May '92, *to be published in the Proceed. IXth Int'l Workshop on Photon-Photon Collisions, March '92, Univ.California, San Diego.*
- [9] DELPHI Collaboration, P.Aarnio et al., Nucl. Instrum. Methods A**303** (1991) 233.
- [10] L.M.Barkov et al., Nucl. Phys. B **256** (1985) 365.
- [11] L.Bergström, R.W.Robinett, Preprint USITP-90-05, Dep.Physics, University of Stockholm, and PSU/TH/64, Dep.Physics, The Pennsylvania State University
- [12] DELPHI Collaboration, DELPHI event generator and detector simulation - User guide, DELPHI note 89-76 (1989), unpublished.
- [13] F.A.Berends, W.Hollik and R.Kleiss, Nucl. Phys. B **304** (1988) 712.
- [14] J.E.Campagne and R.Zitoun, Zeit. Phys. C **43** (1989) 469.
- [15] S.Jadach and Z.Was, Comp. Phys. Comm. **36** (1985) 191.
- [16] T.Sjöstrand, Comp. Phys. Comm. **28** (1983) 229.
- [17] P.Privitera, *Study of the decay  $\tau \rightarrow 3\pi(n\gamma)\nu_\tau$  with the DELPHI Detector at LEP*, Ph.D. thesis, Institut für Experimentelle Kernphysik, Universität Karlsruhe, January, 1993.
- [18] DELPHI Collaboration, P.Abreu et al., Zeit. Phys. C **53** (1992) 41, updated on DELPHI note 92-82 PHYS 193 (1992), submitted to the Int'l High Energy Physics Conference, Dallas, August '92.

## Figure captions

**Figure 1.** Sum of the momenta of the charged particles.

**Figure 2.** Invariant mass of the 3 nearest charged particles, for events with only four tracks and total charge zero. The solid line represents the data, the dashed line represents the Monte-Carlo for the simulation of  $\tau^+\tau^-$  background, and the dotted line represents the Monte-Carlo for the signal for a luminosity corresponding to hundred times the luminosity of the data sample.

**Figure 3.** Smallest invariant mass (assuming the same azimuthal angle) of all possible combinations of two charged particles. The solid line represents the data, and the shaded region represents the Monte-Carlo for the signal for a luminosity corresponding to ten times the luminosity of the data sample.

**Figure 4.** Distribution of the centre of mass energy for the  $e^+e^-V$  and  $\mu^+\mu^-V$  (a) and  $\tau\tau V$  (b) candidate events.

**Figure 5.** Distribution of the  $V$  invariant mass for the  $e^+e^-V$  and  $\mu^+\mu^-V$  (a) and  $\tau\tau V$  (b) candidate events (line), compared to Monte-Carlo simulation for the signal (shaded).

**Figure 6.** Distribution of the invariant mass of the  $\ell^+\ell^-$  pair for the  $e^+e^-V$  and  $\mu^+\mu^-V$  (a) and  $\tau\tau V$  (b) candidate events (line), compared to Monte-Carlo simulation for the signal (shaded).

**Figure 7.** Distribution of the energy of the  $V$  for the  $e^+e^-V$  and  $\mu^+\mu^-V$  (a) and  $\tau\tau V$  (b) candidate events (line), compared to Monte-Carlo simulation for the signal (shaded).

**Figure 8.** Display of the  $\tau^+\tau^-V$  event with higher mass for the  $V$  ( $17.5\pm 0.2$  GeV/ $c^2$ ). The particles composing the  $V$  appear on the left side, giving hits in the outer layers of the muon chambers, classifying the particles as muons. On the right side, a cluster of three charged particle tracks with invariant mass lower than 1.7 GeV/ $c^2$ , and a well separated track with associated hadronic energy are seen, identifying the event as  $\tau^+\tau^-V$ . The energy in the centre of mass is 89.5 GeV, the mass of the  $V$  is  $17.47\pm 0.17$  GeV/ $c^2$ , and the mass of the  $\tau^+\tau^-$  system is  $25.8\pm 0.8$  GeV/ $c^2$  (the mass of the system recoiling from the  $V$ ). Other characteristics can be found in table Ib) (event 28271/3370).

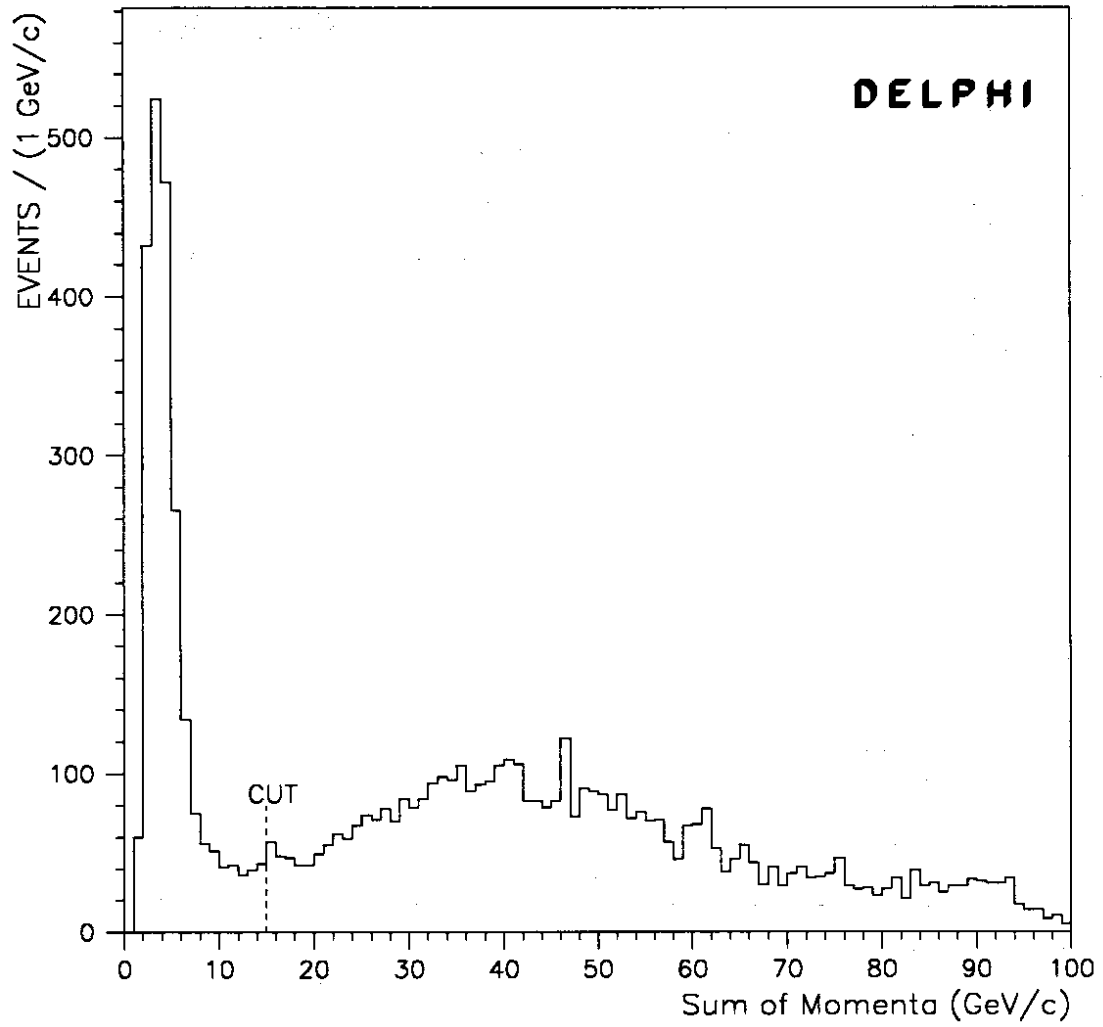


Figure 1:



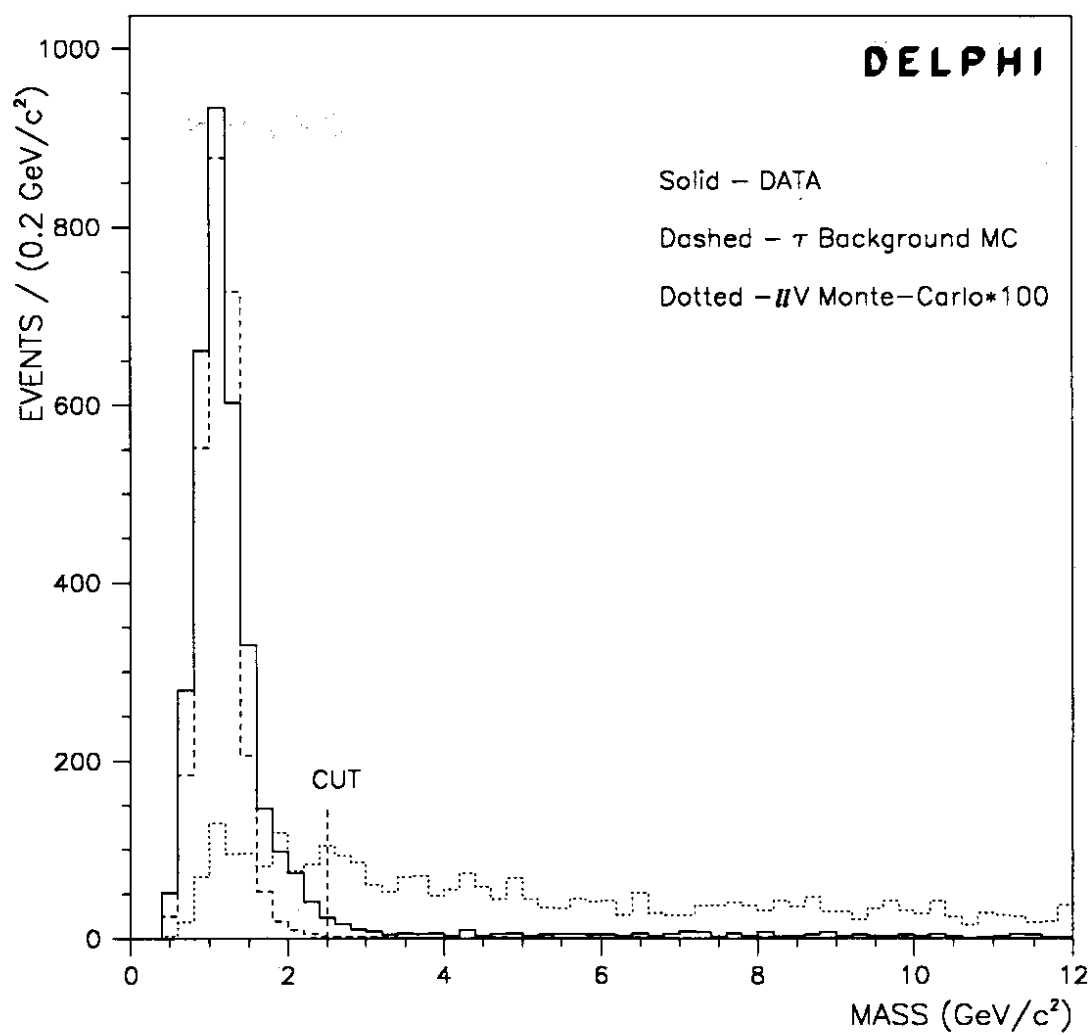


Figure 2:

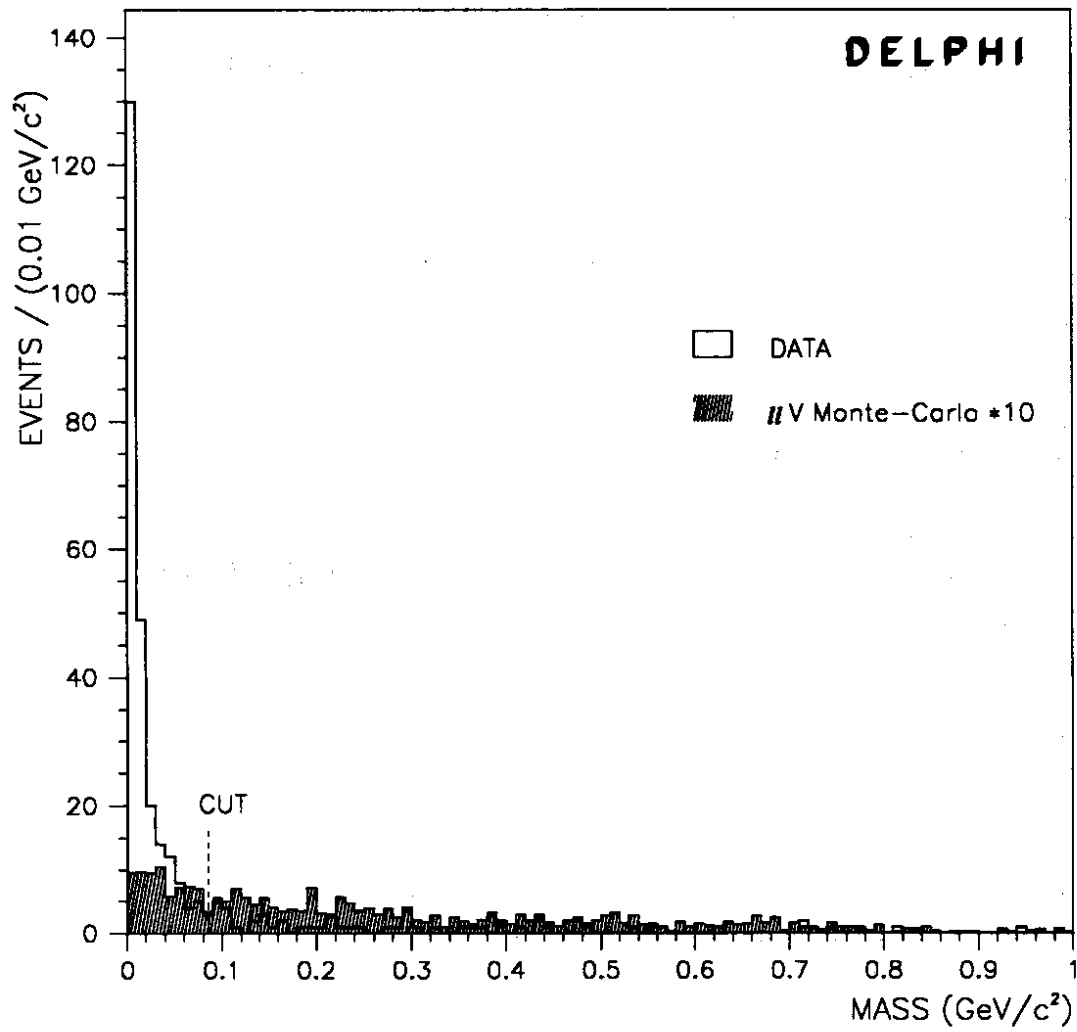


Figure 3:

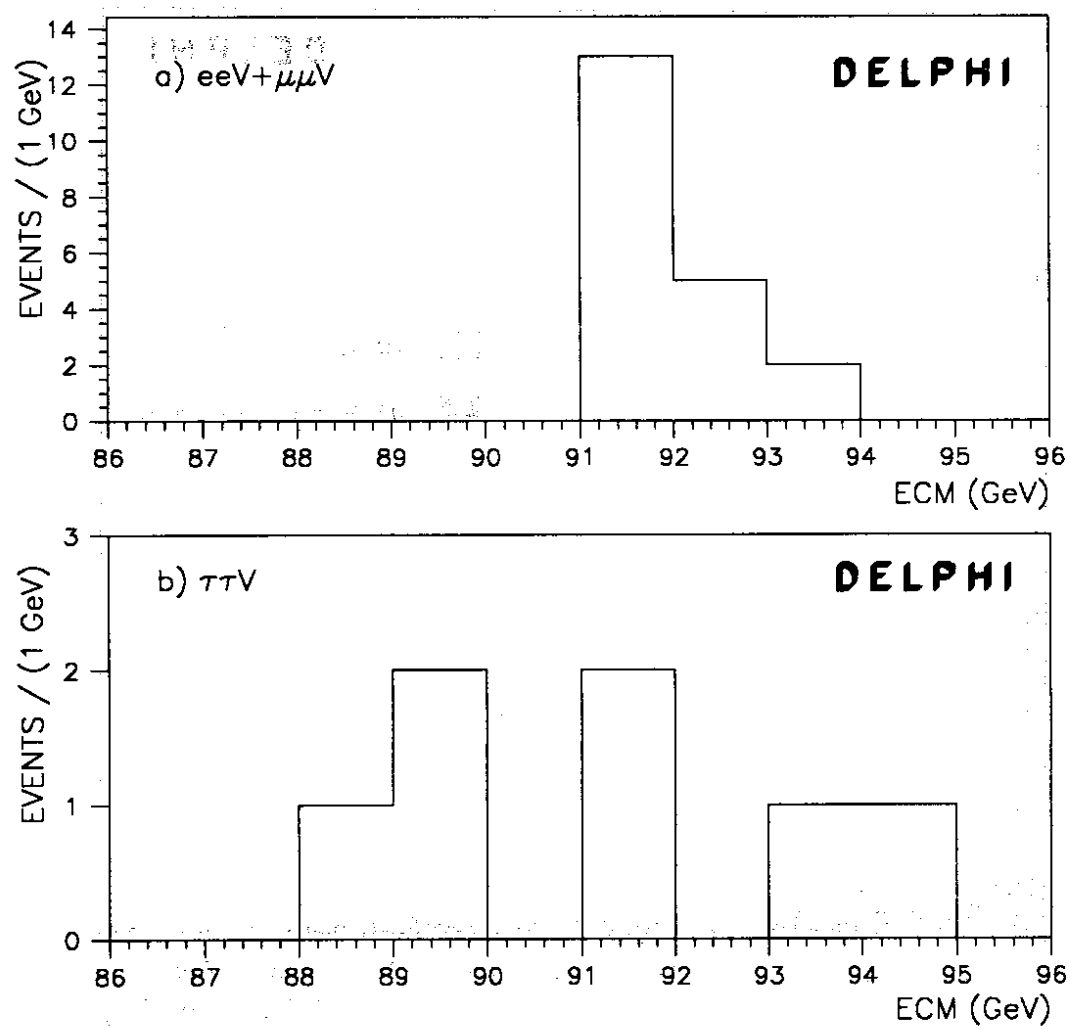


Figure 4:

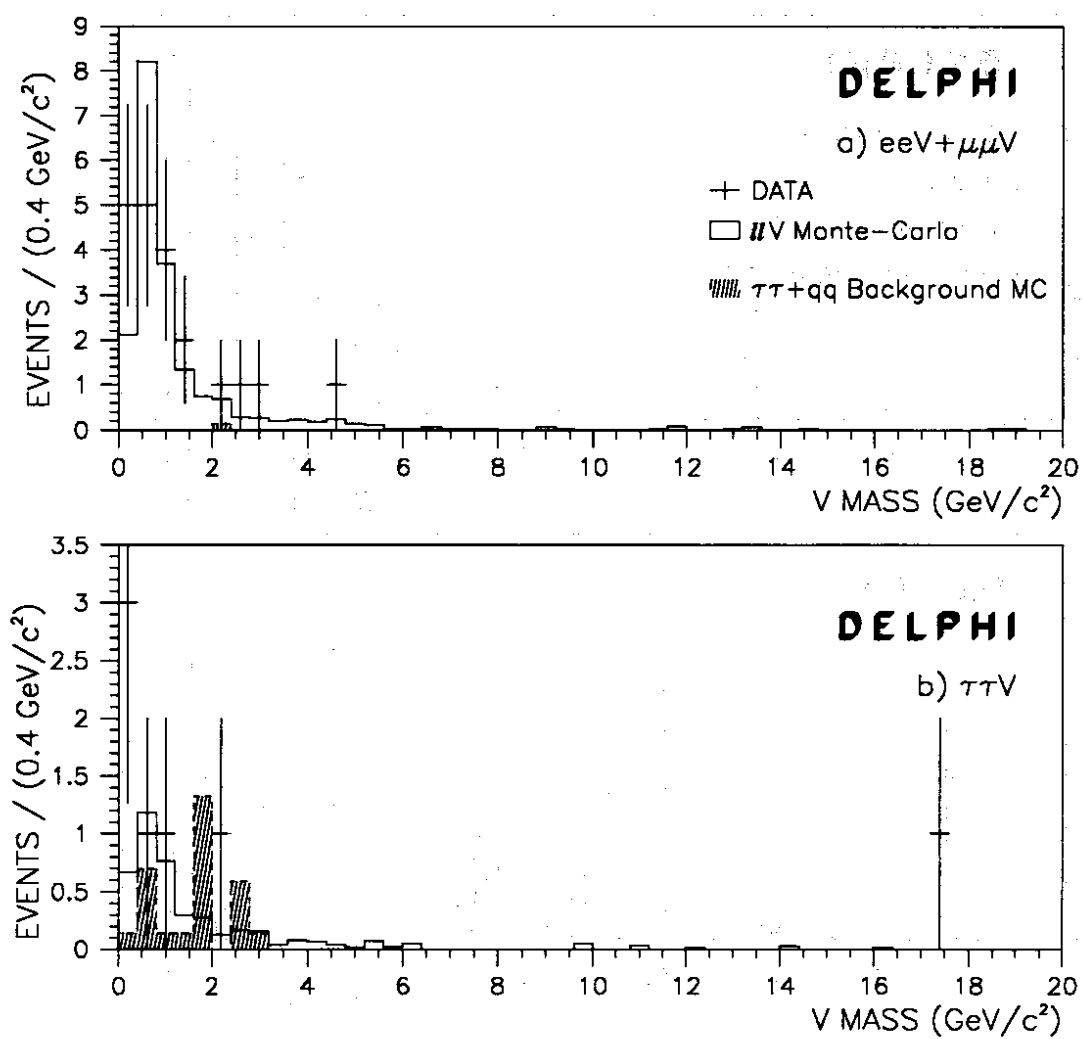


Figure 5:

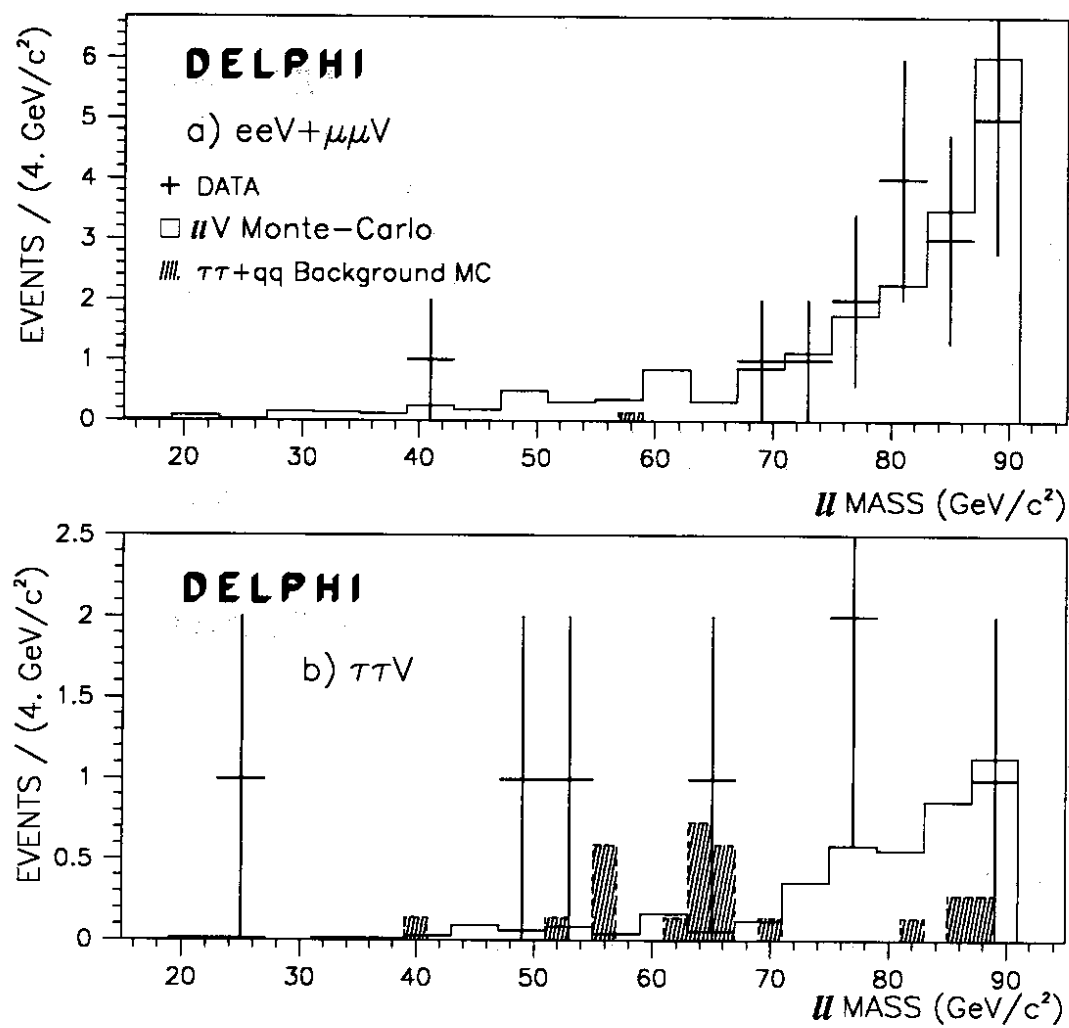


Figure 6:

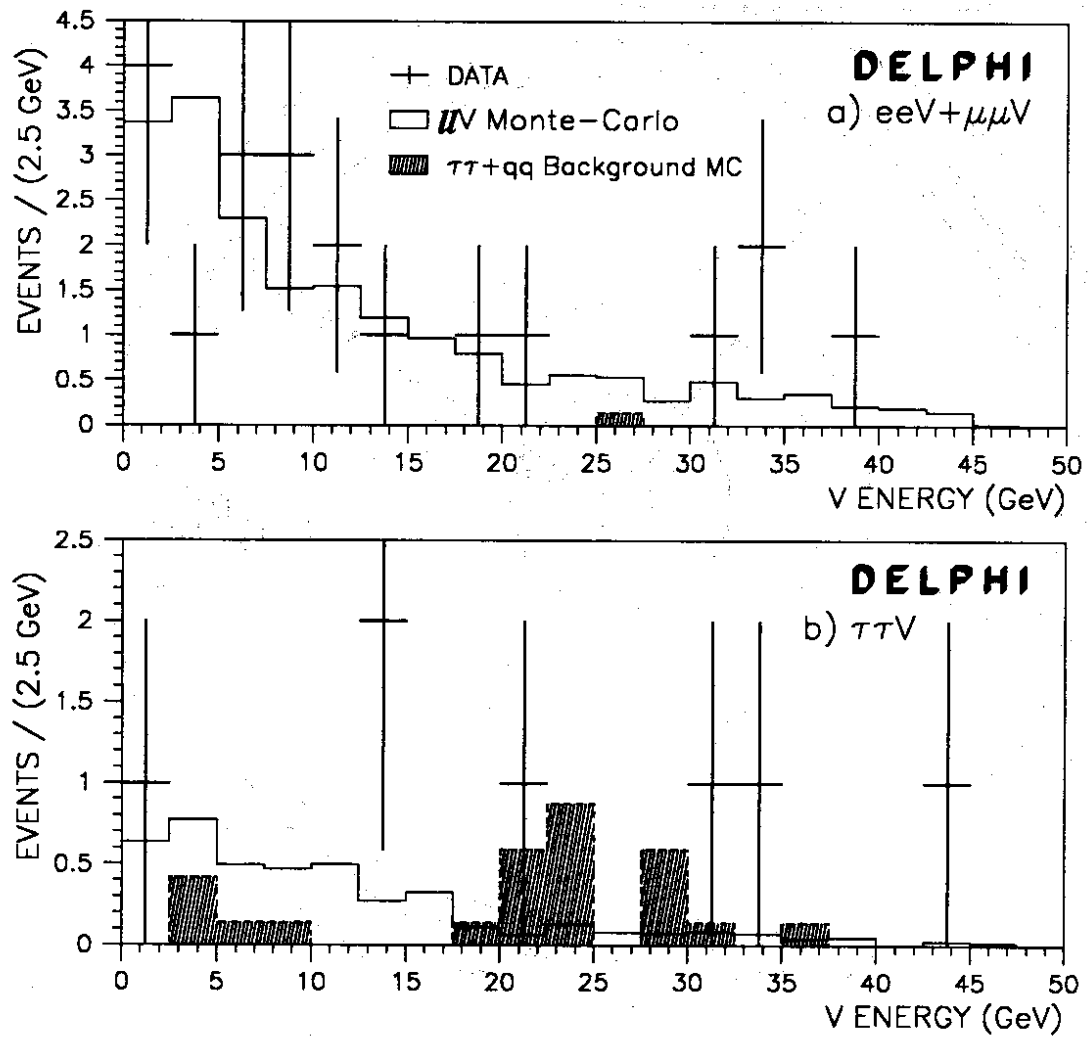


Figure 7:

